International Journal of Engineering

Numerical Study on Flexural Behavior of Concrete Beams Strengthened with Fiber Reinforced Cementitious Matrix Considering Different Concrete Compressive Strength and Steel Reinforcement Ratio

Z. R. Aljazaeri*, Z. Al-Jaberi

Civil Engineering Department, Al-Nahrain University, Baghdad Governorate, Iraq

PAPER INFO	ABSTRACT
	Concrete structures retrofitted with fiber reinforced cementitious matrix (FRCM) have become widespread due to their mechanical and durability performances. However, the behavior of FRCM - strengthened RC members under service loads is still a concern, and more efforts need to be done. In this study, a nonlinear three-dimensional finite element (FE) model has been developed to study the performance of reinforced concrete (RC) beams strengthened by (FRCM). The model was validated against the experimental results gathered from six beams tested under three-points bending. Consequently, the primary numerically studied parameters were longitudinal steel reinforcement ratio and concrete compressive strength. A cohesive damage parameters were investigated to represent the experimental results. Also, the theoretical flexural capacity of strengthened beams based on ACI-549.4R code was evaluated based on the numerical method results. As a conclusion, the numerical results are in a very good agreement with the experimental ones regarding yielding load, ultimate load, and failure mode. In addition, the developed models from parametric studies concluded the insignificant effect of concrete compressive strength on increasing the ultimate capacity of strengthened beam. However, the steel reinforcement ratio has a major impact on enhancing the ultimate capacity of strengthened beams.

NOMENCLATURE

E_c	Concrete modulu of elasticity	M_n	Nominal flexural strength at section
f'_c	Specified compressive strength of concret	M_s	Steel flexural strength at section
f_{ct}	Conceret tensile strength	σ_c	Extreme fiber concret compressive stress
M_f	Fiber flexural strength at section	ε_c	Extreme fiber concret compressive strain

1. INTRODUCTION

During the last decade, FRCM composite material was developed with almost the same advantages of FRP strengthening technique such as high strength to weight ratio, corrosion resistant, and ease of implementation in addition to that to overcome some of the FRP drawbacks specially those related to fire resistance or installing on wet surfaces issue [1-2]. The other physical benefits of FRCM strengthening system are good reversibility and good vapor permeability in addition to consider the

matrices not toxic material like the epoxy that utlized in FRPs technique [3-5].

On behalf of that, many experimental studies have been investigated the structural and durability performances of FRCM material as a strengthening or a repairing system for infrastructural members and compared with structures strengthened with FRP. The experimental works concluded the effectiveness of the FRCM material in increasing the ultimate flexural or shear loads of reinforced concrete (RC) beams/slabs and masonry walls (references of different aspects)[6-10]. Also, the FRCM material was used to improve the

*Corresponding Author Institutional Email: zracnb@mst.edu (Z. R. Aljazaeri)

confinement of RC columns, repairing corroded RC beams, and seismic upgrading for other structural elements [11-13].

Most of the previous studies focused on theoritical and numerical studies of structures strengthened with FRP systems [14-17]. A numerical finite element analysis of RC beams strengthened with EB-FRP techniques was implemented [18]. According to this study, the validated model was able to predict maximum load capacity, load-deflection curves, and the bond slib behavior for both interfaces (FRP-epoxy resin and the epoxy resin with substrate. Furthermore, parametric study was conducted to evaluate many factors and their impact on the efficiency of strengthened RC beams. Recent advances in the use of FRCM material has highlighted the need to carry out reliable numerical analyses based on FE models to predict the strengthening or repairing behavior of FRCM composite with different variables. However, a few FE studies have been modeled structural elements strengthened with FRCM material. To the authors' best knowledge, the studies by D'Ambrisi [4] and Ombres [19] were the only ones found in the literature on this topic. D'Ambrisi et al. [4] conducted a nonlinear FE model for RC beams strengthened with FRCM composite under flexural loads. A perfect bond between the PBO-fibers and concrete was assumed. The numerical load-deflection curves were fit the experimental ones up to a certain point then the theoretical curves began to diverge. So the adopted models did not present the FRCM debonding failure mechanism. Ombres et al. [19] also modeled FRCM strengthened RC beams in flexural by assuming a perfect bond between the FRCM composite and concrete substrate. The numerical results were provided non-accurate predictions for load-deflection relations concerning to the experimental ones. As well, both the ultimate capacity and debonding strains of the numerical model differed in a range of 3 to 40% from that of the experimental work. On the other hand, several FE studies were conducted a single-lap direct shear test to characterize the bond-slip relation between FRCM composite and concrete substrate. D'Antino et al. [20] analyzed the axial strain profiles of the FRCM composite-concrete interface to investigate the stress-transfer mechanism at the matrix–fiber interface. The ultimate debonding load was predicted using the expected fracture parameters from the strain profiles of seven tested specimens. The ultimate loads were in good agreement with the experimental applied loads. Focacci et al. [21] used an indirect method to define interfacial shear stress-slip relation between FRCM composite and concrete substrate. Different cohesive material laws were adopted and calibrated to simulate successfully the experimental load responses. Carloni et al. [22] used a fracture mechanic approach to account for the mixed failure modes observed in the single-lap shear test. The

FE outcomes presented the experimental load responses correctly and imitated different experimental failure modes. D'Antino et al. [23] proposed an analytical model to define the bond behavior of the FRCM-concrete interface using trilinear cohesive material laws based on the experimental results of the single-lap shear test. The proposed model revealed the load response of the FRCM-concrete interface up to the peak stress with sufficient accuracy. However, the proposed model did not present the post-peak behavior of the FRCM-concrete interface. Zou et al. [24] defined a new bond-slip equation for FRCM-concrete joints based on longitudinal fiber strains. The ultimate debonding load showed good agreement with the test results of seven single-lap shear specimens. Despite all these efforts, no full bond-slip relation was proposed and standardized for the FRCM-concrete interface. On the other hand, no numerical studies conducted to validate the use of the proposed bond-slip laws in analyzing structural members strengthened with FRCM composite. There is a lack of experimental researches on the flexural behavior of RC beams strengthened with FRCM under different concrete compressive strength or longitudinal steel reinforcement ratio. This paper aims to fill these gaps numerically by presenting the results of theses factor through validated model. Validated FE models can be very robust analytical tool, since it will typically result in enormous reductions of time and cost.

2. SIGNIFICANCE AND OBJECTIVES

In many instances, flexural concrete members sustain damage due to excessive load or harsh environmental conditions and therefore require rehabilitation and upgrade, conventionally by using advanced composite such as NSM-FRP bars or EB-FRP sheets. The second generation of advanced composite (FRCM system) has several distinct properties that provides the advantages of FRP technique in addition to eliminate the problems related to organic adhesive.

The behavior of FRCM technique in strengthening RC beams considering different types of open mesh fibers, or concrete has not been fully examined and understood. The objective of this paper is to assess the applicability of cohesive bond model (CBM) in modeling FRCM strengthened beams under flexural loads and to propose and validate a robust, non-linear (FE) model that used to predict the behavior of strengthened beams considering different parameters. The validated model is used mainly to examine key parameters that have not been studied yet, including: different compressive strength of concrete, ranging from normal to high strength and longitudinal steel reinforcement ratio, ranging from (0.24 to 1.06%). Knowing the influence of these key parameters on the structural performance of

strengthened beams with FRCM composite would assist in advanced applications and provide a design clue for different cases that have not been touched experimentally. It should be noticed that the various steel reinforcement ratio was used to evaluate the accuracy of ACI 549.4R total flexural capacity equation.

3. SUMMARY OF EXPERIMENTAL PROGRAM

The RC concrete beams tested by Babaeidarabad et al. [3] were selected to validate the predictions of the FE model developed in this study. Six RC beams were tested under three- points bending. Three beams made of low-strength and the other three made of high-strength concrete. The low and high compressive strength were represented the range of compressive strength of fabricated beams in the last decades. So based on ACI 363R [25], the concrete with compressive strength of 34 MPa (5000 psi) was considered high strength. Nowadays, these beams are in need of repair and strengthen to meet the new requirement of building codes and retain back to service.

All the beams had a rectangular cross-section of 152 mm*260 mm and a length of 1,829 mm with a clear span of 1,524 mm. The six beams were reinforced with 2-13 mm diameter longitudinal steel bars at the tension and compression faces and 10 mm diameter transverse reinforcement spaced at 127 mm. Typical beam layout and corss-section is presented in Figure 1.

The specimen identification system consisted of two parts as summarized in Table 1. The first part represented concrete information, L for Low compressive strength and H for high compressive strength concrete. The second part identifies the number of open mesh layers. In case of reference specimen, the second part denoted as control.

4. FINITE ELEMENT MODEL DEVELOPMENT

4. 1. Model Description
Finite element analysis was performed the nonlinear behavior of RC beams strengthened with FRCM composite using Abaqus 6.14

TABLE 1. Experimental test matrix

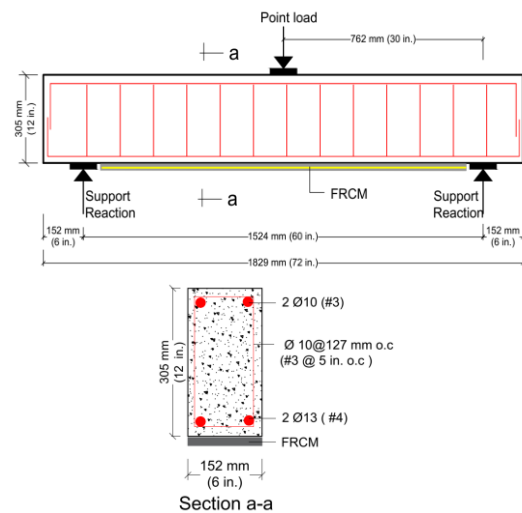| Specimen ID	Type of concrete	Number of layers
L-control	Low compressive strength	-
L-1ply	Low compressive strength	1
L-4ply	Low compressive strength	4
H-control	High compressive strength	-
H-1ply	High compressive strength	1
H-4ply	High compressive strength	4

Figure 1. Beam layout and its cross-section

/standard [26]. The full length of tested beams was simulated to recognize the failure mechanism of FRCM composite along the beams. A three-dimensional finite element mesh is shown in Fig. 2. A fine mesh of approximate global size (25 mm) was selected to ensure sufficient accuracy in the numerical results. Also, the selected meshing size providing a good balance between accuracy and the cost in terms of desk space and running time. The boundary conditions were set in the middle of supporting plates. A simply-supported boundary was considered in the x and y directions, respectively. The roller support boundary was constraint in the x-direction only. The load was induced by the deflection-controlled method in order to simulate the post-peak behavior. The number of loading steps was 100 step. The total applied load was equal to the sum of two vertical reactions associated with each loading step.

4. 2. Types of Elements
The beam element C3D8R was adopted for both concrete and steel plates that used under loading and supporting points. The truss element T3D2 was adopted for modeling the steel reinforcement (longitudinal and transverse reinforcement). The steel reinforcement was embedded inside the concrete beam. This type of bonding did not include the effect of slip between the reinforcement and concrete beam. Instead, these properties were partly considered through the definition of concrete tension softening. The shell element S4R was adopted for FRCM composite. The loading and supporting plates were tied to the concrete beam by surface to surface contact.

4. 3. Material Models
The compressive behavior of concrete material was first characterized by a linear elastic behavior and second by a nonlinear plastic behavior (Figure 3a). The linear elastic behavior was
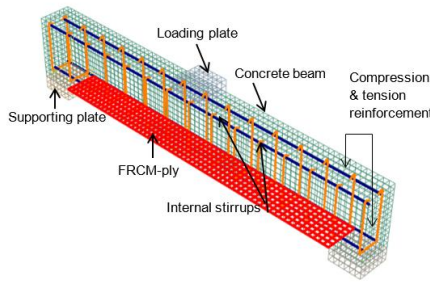
Figure 2. Typical 3D finite element mesh model for the strengthened beam

defined by the elastic modulus (25 GPa) based on Equation (1) [27] and Poisson's ratio (0.2). A plastic damage model presented the plastic compressive behavior of concrete material. This model had two failure modes (tensile cracking and compressive crushing) [24]. The plastic damage model of concrete defined by the plastic damage parameters, density, and post-peak tensile/compressive behavior. The five damage parameters were the dilation angle (30), the flow potential eccentricity (0.1), the ratio of initial biaxial compressive yield stress to initial uniaxial compressive yield stress (1.16), the ratio of the second stress invariant on the tensile meridian to that on the compressive meridian (0.667), and the viscosity parameter (0.001). The concrete density (2400 kg/m³) was considered. The compressive behavior of concrete was modeled by the stress-strain relation in Equation (2) [28]. The peak concrete strain was assumed to equal 0.0025 mm/mm and the ultimate concrete strain was equal to 0.003 mm/mm [3]. The tensile behavior of concrete material consisted of two phases (Figure 3b). The first phase presented the linear elastic behavior of concrete up to reaching its tensile strength. The second phase presented the descending branch in the uniaxial tensile stress-strain relation due to crack occurrence and its propagation in concrete material. The ultimate tensile strength of concrete was estimated by Equation (3) [28]. The second phase was assumed as a linear softening branch where the ultimate tensile strain at the end softening was set to be 0.001 mm/mm. The degradation in the concrete stiffness was simulated by concrete damage parameters (d_c in compression and d_t in tension)
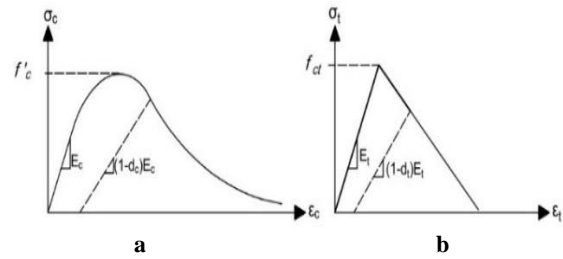
$$E_c = 4700\sqrt{f'_c} \qquad (1)$$

where f'_c is given in MPa.

$$\sigma_c = \frac{E_C\,\varepsilon_c}{1+(R+R_E-2)\left(\frac{\varepsilon_c}{\varepsilon_0}\right)-(2R-1)\left(\frac{\varepsilon_c}{\varepsilon_0}\right)^2 + R\left(\frac{\varepsilon_c}{\varepsilon_0}\right)^3} \qquad (2)$$

where

$$R = \frac{R_E\,(R_\sigma-1)}{(R_\varepsilon-1)^2} - \frac{1}{R_\varepsilon}, \quad R_E = \frac{E_C}{E_0}, \; E_0 = \frac{f'_c}{\varepsilon_0} \text{ and}$$

Figure 3. The behavior of concrete in uniaxial loadings: (a) compression; and (b) tension

$$\varepsilon_0 = 0.0025, \; R_\varepsilon = 4, \; R_\sigma = 4, \; \text{as reported in [28]}$$

$$f_{ct} = 0.33\sqrt{f'_c} \qquad (3)$$

The steel reinforcement was simulated as an elastic-plastic material. In the linear elastic range, the behavior was defined by the young modulus (190,000 MPa) and the Poisson's ratio (0.3); whereas in the plastic range, the density (7800 kg/m³) and the yield strength (276 MPa) were defined. The elastic-plastic properties of steel reinforcement were based on the results of coupon tests [3]. The ultimate plastic strain was assumed 0.015 mm/mm.

The FRCM composite consisted of the polyparaphenylene benzobisoxazole (PBO) fabric with a cement based curing agent. The width of PBO-fabric was 5 mm and 10 mm in the longitudinal and transverse directions, respectively. The free spacing between the strands was approximately 5 mm and 15 mm in the longitudinal and transverse directions, respectively. The two dimensional mesh of PBO fabric were embedded inside the cement based (matrix) that produced the FRCM composite. The interaction between the PBO-fabric and the cement matrix were represented by a cohesive element having initial elastic stiffness (k_0) in kN/mm, maximum shear stress (τ_{max}) $in\ MPa$, and fracture energy (G_f) in N/mm, are ranged between (1.5-9.85), (0.2-1.5), and (0.4-5); respectively.

The FRCM composite was modeled as a laminate. The FRCM composite' tensile properties were based on coupon tests reported by Babaeidarabad et al. [3]. The input parameters were: the modulus of elasticity (128,000 MPa), Poisson's ratio (0.3), and ultimate tensile strength (1,664 MPa). The FRCM laminate properties in the two directions were assumed equally. The FRCM laminate thickness was 5 mm for one-ply and 10 mm for four plies, respectively, all other properties can be found in literature [3].
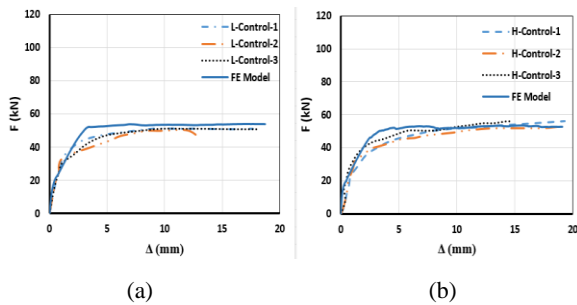
4. 4. FRCM-Concrete Interface Model   The simulation of the interface between FRCM composite and concrete substrate was the critical feature in modeling the strengthened beams. Therefore, different

interfacial bond models were considered here. The cohesive bond model (CBM) was defined by a simple bilinear traction–separation law [26]. The interfacial cohesive behavior was initially linear elastic and followed by a descending linear branch which denoted the initiation of damage. The traction–separation response was described by three failure modes: opening (mode I), sliding I (mode II), and sliding II (mode III). Through literature, many experimental and numerical works have been determined the cohesive damage parameters between the FRCM composite and concrete [13-17] and these values will guide the researcher in the future studies. Based on these studies, the CBM parameters including initial elastic stiffness (k_0) in kN/mm, maximum shear stress (τ_{max}) $in\ MPa$, and fracture energy (G_f) in N/mm, are ranged between (1.5-9.85), (0.2-1.5), and (0.24-1.5); respectively.
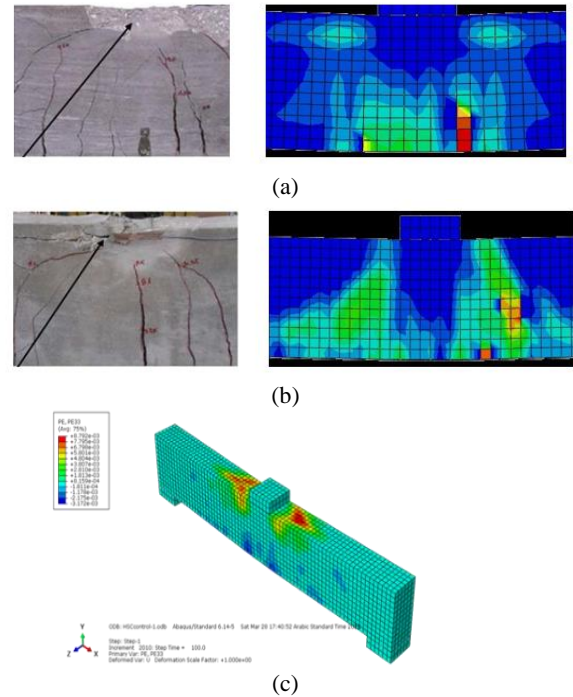
5. MODEL VALIDATION

5. 1. Control Beams The load–midspan deflection curves for control beams from experiments and FE analysis are plotted in Figure 4. The behavior of beams predicted by FE analysis is slightly stiffer and stronger after yielding point due to the assumption of fully bonded between concrete and reinforcement. However, the numerical results for control beams showed a very good agreement with the experimental results in term of load deflection curves. This agreement indicates that the constitutive models used for concrete and reinforcement were effectively captured the flexural behavior of RC beams. The concrete cracks that exhibited in the experimental and numerical models were compatible. The failure mode for both control beams was indicated by yielding of the tension reinforcement followed by concrete crushing at the mid-span section as experimentally observed in Figures 5a and 5b.

Its worthy to mention that the finite element model shows the plastic strains in the tension face of the beam in a separate view from the compression face. The compression face damage is shown Figure 5c. Where

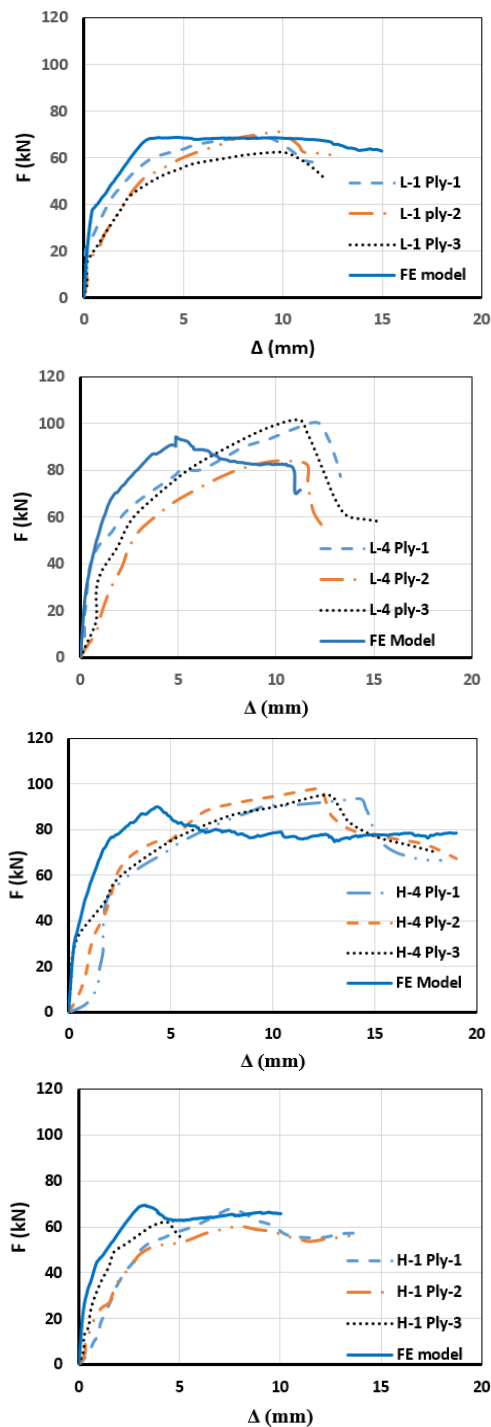**Figure 5.** Experimental/numerical failure modes for (a) L-control, (b) H-control, (C) compression face damage

the concrete crushed near the loading point in the compression fiber face.

The model was verified with additional work defined by Aljazaeri and Myers [2]. The finite element models were found to be compatible with the experimental test results. The ultimate load capacities for the modeled beams were compatible by 100% with the experimental tested control beam and 90% with the strengthened beam. However, the ultimate displacements for the modeled beams were compatible by 100% with the experimental tested control beam and 80% with the strengthened beam.

5. 2. Strengthened Beams The cohesive bond model was selected to simulate the load-midspan deflection responses of strenfthened beam since the previous studies proved that the perfect bond model was not able to simulate that accurately. The load–midspan deflection curves for strengthened beams from experiments and FE presented in Figure 6. All modeled beams showed very close results of yielding and ultimate loads in comparison with the experimental ones. For the purpose of relability, the FE model was also verifed based on Aljazaeri and Myers work [2] and close results were determined.

A comparison between the numerical and experimental results at the yielding stage and ultimate stage in terms of loads and deflections are given in Tables 2 and 3.

Figure 4. Comparison between experimental results and FE results for control beams: (a) L-control; and (b) H-control

Figure. 6. Comparison between experimental results* and FE results of modified CBMs for strengthened beams: (a) L-1ply; (b) L-4ply; (c) H-1ply; and (d) H-4ply

TABLE 2. Test results: experimental and numerical load

Specimen ID	Experimental		Numerical		Difference	
	P_y (kN)	P_u kN)	P_y (kN)	P_u (kN)	$\dfrac{P_{y,(num.)}}{P_{y,(exp.)}}$	$\dfrac{P_{u,(num.)}}{P_{u,(exp.)}}$
L-control	38	51.4	39	54	1.03	1.05
L-1ply	57	67.7	57	68.9	1.00	1.02
L-4ply	75	99	77	84.5	1.03	0.85
H-control	40	55.8	42	53.5	1.05	0.96
H-1ply	54	63	58	69.6	1.07	1.10
H-4ply	78	96.8	81	90	1.04	0.93

TABLE 3. Experimental and numerical midspan deflection

Specimen ID	Experimental*		Numerical		Difference	
	δ_y (mm)	δ_u (mm)	δ_y (mm)	δ_u (mm)	$\dfrac{\delta_{y,(Num.)}}{\delta_{y,(Exp.)}}$	$\dfrac{\delta_{u,(Num.)}}{\delta_{u,(Exp.)}}$
L-control	1.4	25	1.9	25	1.36	1.00
L-1ply	2.3	12	2	12	0.87	1.00
L-4ply	3.3	12.2	3.3	4.4	1.00	0.36
H-control	1.6	24	2	24	1.25	1.00
H-1ply	2.4	5.5	2	3.5	0.83	0.64
H-4ply	3.8	15	2.8	4.5	0.74	0.30

were in excellent agreement with the corresponding experimental results. As well, the modeled beam (L-1ply) failed by slippage of the PBO-fiber as observed experimentally. The strengthened beam with 4 layers (L-4ply) (Figure 6b), the modeled beam was underestimated the ultimate load by 15%. However, the descending curve represented the debonding failure in the FRCM plies as exhibited experimentally.

The comparison between experimental and FE load-midspan deflection curves for high strength concrete strengthened with one and four layers of FRCM are presented in Figures 6c and 6d. It can be seen that the FE model was able to represent the strengthened beam behavior with a good level of accuracy. The ultimate load values predicted from FE models were within 15% and 7 % as a maximum divergence from the experimental values for beams strengthen with one and four layers, respectively. However, stiffer load-midspan deflection responses tolerated the yielding and ultimate deflections specifically for strengthened beams with four plies.

6. FAILURE MODES AND STRAIN MEASUREMENTS

In order to increase the reliability of the FE model, the local measurement of a strain gage at the mid-span of beam, and observing mode of failures were compared

The CBM precisely simulated the experimental load-midspan deflection response of both low and high strength concrete. For the beam with low compressive strength and strengthened with one layer (L-1ply), the ultimate load, initial stiffness and ultimate deflection

with the corresponding FE value. The CBM was able to present the experimental failure modes of control and strengthened beams. The control beams detected a yielding of steel reinforcement with ductile failure as experimentally observed [3]. The strengthened beam with one FRCM ply failed by yielding of tension steel reinforcement followed by PBO-fibers' slippage (Figure 7a). While debonding of FRCM plies were detected in strengthened beams with four plies (Figure 7b).

The strain measurements of tested beams perceived by CBM were compared with the experimental results. Table 4 presented the numerical strain measurements for concrete, internal steel reinforcement, and FRCM composite at the beams' midspan.

All the modeled beams observed strain measurement of concrete that was equal approximately to the experimental ultimate strain (0.003 mm/mm). The numerical strain measurements of the internal steel reinforcement for the control and strengthened beams were agreed with the experimental ones. The numerical strain of the internal reinforcement ranged between (0.006 mm/mm to 0.009 mm/mm) for strengthened beams and (0.025 mm/mm to 0.07 mm/mm) for control beams, as observed experimentally [3].

However, the numerical strain measurements of FRCM composite were not compatible with the experimental ones. Since the experimental strain measurement was referred to the maximum strain in the PBO-fiber, but the numerical strain measurement referred to the maximum strain in FRCM composite as a laminate. In summary, it is observed that the CBMs revealed close numerical results to the experimental results for strengthened beams with one ply. In contrast, the numerical results of strengthened beams with four plies were far from the experimental results. The reason behind that the CBMs were dependent on tested specimens with one FRCM ply so CBMs did not account for four FRCM plies.

The numerical results found here were agreed with the previous studies' results reported by Elghazy et al.
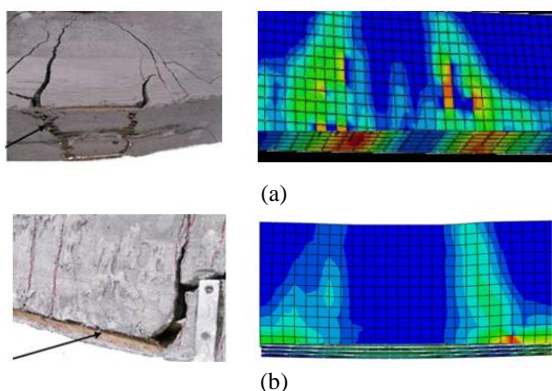
Figure. 7. Experimental/numerical failure modes: (a) L-1ply; and (b) L-4ply

TABLE 4. Numerical strain measurements

Specimen ID	Strain at midspan, mm/mm		
	Concrete	Steel	FRCM composite
L-control	0.003	0.07	-
L-1ply	0.002	0.008	0.001
L-4ply	0.001	0.006	0.002
H-control	0.003	0.025	-
H-1ply	0.005	0.008	0.001
H-4ply	0.004	0.009	0.003

[12] where the ultimate loads and failure mechanism can be captured by CBMs but still, the numerical load-midspan deflection responses were varied from the experimental ones. Thus, new bond-slip laws need to address the increase in FRCM plies and denote precisely the cohesive damage parameters in the normal (mode I) and shear (mode II, III) directions.

7. PARAMETRIC STUDY

A comprehensive parametric study was conducted using the validated model. A total of 10 new models was used to study the effects of key variables that expected to have an essential impact on the behavior of strengthened RC beams. These parameters were the longitudinal steel reinforcement ratio and concrete compressive strength. For each key variable, both control and strengthened models were constructed in order to evaluate the contribution of open mesh fiber on the examined parameters. The observations for different parameters are described as follow:

7. 1. Longitudinal Steel Reinforcement Ratio A total of four FE models were conducted to evaluate the effect of steel reinforcement ratio (ρ) on the flexural behavior of RC beams strengthened with one layer of PBO fiber. For all models, concrete with normal compressive strength was used and four different sizes of steel reinforcement bars (2#12, 2#16, 2#20 and 2#25 mm bars) that equivalent to steel reinforcement ratio (ρ) of 0.24, 0.43, 0.67, and 1.05%; respectively.

The developed FE models results are presented in Table 5. In addition, Figure 8 compares the improvement of ultimate load of the strengthened beams with the control beams for different steel reinforcement ratio. As the reinforcement ratio increased a significant enhancement from strengthening can be achieved.

The results showed that all specimens failed by slippage in PBO also the post crack stiffness was increased with the increasing of steel reinforcement ratio which led to increase ductility of the specimens.

TABLE 5. Effect of different steel reinforcement ratio

Steel reinforcement ratio (%)	Ultimate load, Pu (kN)	Ultimate deflection (mm)	Post crack stiffness, k (kN/mm)
0.24	89	6.34	15.4
0.43	114	8.65	17.3
0.67	123	5.25	24
1.05	126	5.62	39
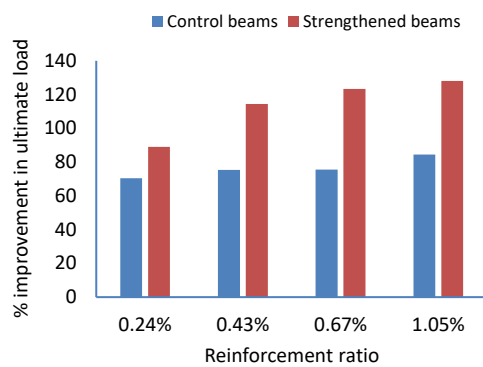
Figure 8. The improvement of ultimate load in different steel reinforcement ratio.

The FE results for flexural strengthened beams are compared with the analytical approach considering the ACI 549.4R code [9] in order to evaluate this approach under different steel reinforcement ratios as shown in Table 6. Based on ACI 549.4R [9], the flexural strength is calculated in accordance with Equation (4)

$$M_n = M_s + M_f \qquad (4)$$

where M_n is the nominal flexural capacity of strengthened beam, and M_s and M_f are the contribution of internal steel reinforcement and external advanced composite material.

From Table 6, its observed that the results from the analytical model of ACI 549.4R [9] was very close to the results of FE models. The difference between two approaches within the range 12-25%. The reason behind this difference is the analytical model supposed uncoupled contribution of the steel and fiber which is not the case in FE models.

7. 2. Concrete Compressive Strength   A total of six FE models were developed to study the effect of concrete compressive strength on the flexural behavior of strengthened beam. All beams had a constant external open mesh fiber (one layer of PBO) and internal reinforcement ratio of 0.24%. The concrete compressive strength was varied from 20 MPa to 50 MPa. The FE results are summarized in Table 7.

TABLE 6. Comparison between FE and analytical results

Steel reinforcement ratio (%)	ultimate load (kN) based on FE	ultimate load (kN) based on analytical method
0.24	89.05	78.81
0.43	114.33	112.09
0.67	123.35	170.34

TABLE 7. Effect of different concrete compressive strength

Concrete compressive strength (MPa)	Ultimate load, Pu (kN)	% Pu increase over control beams	Ultimate deflection (mm)	Uncracked stiffness (kN/mm)
20	66.5		3.8	85
25	67.7	102%	4	87
30	68.9	104%	5	89
35	70	105%	4.7	91
40	70	105%	3.1	94
50	71.4	107%	2.9	100

The load-deflection response was similar for simulated beams with concrete having compressive strength between 20 MPa to 35 MPa. Then, for simulated beams with higher compressive strength, load-deflection response become very brittle. A lower stiffness could be noticed for beams with low concrete strengths. However, the percentage increase in the ultimate loads was limited between 4% and 7%. The reason behind that is due to the fact that the flexural capacity of concrete beams reinforced with under reinforcement amount is dominated by the steel bar yield strength rather than compressive strength of concrete.

The concrete strength influenced the mode of failure in the FRCM strengthened system. For low concrete strength, a slippage of the PBO fiber was observed in the strengthened beams. While strengthened beams having high concrete strength above (35 MPa) observed a debonding failure mode in the FRCM system.

8. CONCLUSIONS

The FE models were developed in this study to analyze RC beams strengthened with FRCM composite under flexural load. The first step of modeling was to consider the cohesive bond models. Based on the result, the cohesive bond model presented good results in term of bond-slip behavior.

After validation with six full-scale RC beam tests, featuring different types of concrete, and different number of open mesh layers, in addition to different 10

other models that was used in a parametric study such as: different longitudinal steel reinforcement ratio and concrete compressive strength. The results showed a good agreement between the developed models and experimental results from uncracked stage till failure. The following conclusions can be drawn here:

1. The developed FE models were able to reasonably predict the flexural performance of RC beams with and without external strengthening with open mesh fibers.

2. The cohesive bond models prove to represent the load-midspan deflection responses of strengthened beams in comparison with their peers that were obtained from experimental work. The predicted yielding loads, ultimate loads, and failure modes are in excellent correlation with the experimental work.

3. The theoretical flexural capacity of strengthened beams based on ACI 549.4R code was evaluated based on numerical results. The developed models showed satisfactory computational capacity since the results of FE models and the theoretical results were close enough.

4. The variation in the concrete compressive strength has not dramatically influence the flexural behavior and the ultimate capacity of strengthened beam since failure mechanism was controlled by the steel bar yield strength rather than concrete compressive strength.

9. REFERENCES

1. Al-Jaberi, Zuhair A., John J. Myers, and Mohamed A. ElGawady. "Evaluation of FRP and FRCM composites for the strengthening of reinforced masonry walls." *Journal of the American Concrete Institute,* Vol. 327, (2018), 32-41. DOI: 10.14359/51702227.

2. Aljazaeri, Zena R., and John J. Myers. "Fatigue and flexural behavior of reinforced-concrete beams strengthened with fiber-reinforced cementitious matrix." *Journal of Composites for Construction,* Vol. 21, No. 1, (2017), DOI: 10.1061/(ASCE)CC.1943-5614.0000726.

3. Babaeidarabad, S., Loreto, G., Nanni, A. "Flexural strengthening of RC beams with an externally bonded fabric-reinforced cementitious matrix", *Journal of Composites for Construction*, Vol. 18, No. 5, (2014). DOI: 10.1061/(ASCE)CC.1943-5614.0000473.

4. D'Ambrisi, A., Focacci, F. Flexural strengthening of RC beams with cement-based composites. *Journal of Composites for Construction,* Vol. 15, No. 5, (2011) 707-720. DOI: 10.1061/(ASCE)CC.1943-5614.0000218.

5. Al-Jaberi, Zuhair A., John J. Myers, and Mohamed A. ElGawady. " Out-of-plane behavior of RM walls strengthed with FRCM composite or NSM with cementitious adhesive." 9th International Conference on Fibre-Reinforced Polymer (FRP) Composites in Civil Engineering, CICE 2018, DOI: 10.14359/51702227.

6. Aljazaeri, Zena R., and John J. Myers. "Strengthening of reinforced-concrete beams in shear with a fabric-reinforced cementitious matrix." *Journal of Composites for Construction,* Vol. 21, No. 5, (2017), DOI: 10.1061/ (ASCE)CC.1943-5614.0000822.

7. Loreto, Giovanni, et al. "Performance of RC slab-type elements strengthened with fabric-reinforced cementitious-matrix composites." *Journal of Composites for Construction,* Vol. 18, No. 3, (2014), A4013003. DOI: 10.1061/(ASCE)CC.1943-5614.0000415.

8. Al-Jabari, Zuhair, John J. Myers, and Mohamed ElGawady. "Effectiveness of FRCM System in Strengthening Reinforced Masonry Walls Subjected to Cyclic Loading." IABSE Symposium Report. *International Association for Bridge and Structural Engineering*, Vol. 109, No. 39, (2017), DOI: 10.1016/j.compstruct.2018.11.085.

9. ACI (American Concrete Institute). Guide to design and construction of externally bonded fabric-reinforced cementitious matrix (FRCM) systems for repair and strengthening concrete and masonry structures. ACI 549.4 R. (2013). Farmington Hills, MI: ACI.

10. Maghsoudi, A. A., Reza Rahgozar, and Seyed Hamid Hashemi. "Flexural testing of high strength reinforced concrete beams strengthened with CFRP sheets." *International Journal of Engineering, Transactions B: Applications,* Vol. 22, No. 2 (2009), 131-146.

11. Ombres, Luciano, and Salvatore Verre. "Structural behaviour of fabric reinforced cementitious matrix (FRCM) strengthened concrete columns under eccentric loading." *Composites Part B: Engineering,* Vol. 75, (2015), 235-249, DOI:10.1016/j.compositesb.2015.01.042

12. Elghazy, M., El Refai, A., Ebead, U., Nanni, A. "Corrosion-damaged RC beams repaired with fabric-reinforced cementitious matrix." *Journal of Composites for Construction,* Vol. 22, No. 5, (2018), 04018039, DOI: 10.1061/(ASCE)CC.1943-5614.0000873.

13. Al-Jaberi, Zuhair, John Myers, and Mohamed ElGawady. "Flexural capacity of out-of-plane reinforced masonry walls strengthened with externally bonded (EB) FRP." 7th International Conference on Advanced Composite Materials in Bridges and Structures Vancouver, British Columbia, Canada. 2016, DOI: 10.1016/j.conbuildmat.2018.02.043.

14. Mohsenzadeh, Sajjad, Ahamd Maleki, and Mohammad Ali Yaghin. "Experimental and Numerical Study of Energy Absorption Capacity of Glass Reinforced SCC Beams." *International Journal of Engineering*, *Transactions C: Aspects*, Vol. 32, No. 12, (2019), 1733-1744, DOI: 10.5829/IJE.2019.32.12C.06.

15. Alferjani , M. B. S., Abdul Samada, A. A., Elrawaffb, B. S. , and Mohamad, N. "Experimental and theoretical investigation on shear strengthening of RC precraced continuous t-beams using CFRP strips." *International Journal of Engineering, Transactions B: Applications,* Vol. 28, No. 5, (2015): 671-676, DOI: 10.5829/idosi.ije.2015.28.05b.04.

16. Al-Jaberi, Zuhair, John J. Myers, and Mohamed A. ElGawady. "Experimental and analytical approach for prediction of out-of-plane capacity of reinforced masonry walls strengthened with externally bonded FRP laminate." *Journal of Composites for Construction,* Vol. 23, No. 4, (2019): 04019026, DOI: 1061/(ASCE)CC.1943-5614.0000947.

17. Fadaee, Mohammad Javad, and Hamzeh Dehghani. "Reliabilty-based torsional design of reinforced concrete beams strengthened with CFRP laminate." *International Journal of Engineering, TransactionsA: Basics,* Vol. 26, No. 10, (2013), 1103-1110.

18. Zhang SS, and Teng JG. "Finite element analysis of end cover separation in RC beams strengthened in flexure with FRP." Engineering structures. Vol. 75, (2014), 550-560, DOI: 10.1016/j.engstruct.2014.06.031.

19. Ombres, Luciano. "Flexural analysis of reinforced concrete beams strengthened with a cement based high strength composite material." *Composite Structures,* Vol. 94, No. 1, (2011), 143-155, DOI: 10.1016/j.compstruct.2011.07.008.

20. D'Antino, T., Carloni, C., Sneed, L. H., Pellegrino, C. "Matrix–fiber bond behavior in PBO FRCM composites: A fracture mechanics approach." *Engineering Fracture Mechanics,* Vol. 117, (2014), 94-111, DOI:10.1016/j.engfracmech.2014.01.011.

21. Focacci, F., D'Antino, T., Carloni, C., Sneed, L. H., Pellegrino, C. "An indirect method to calibrate the interfacial cohesive material law for FRCM-concrete joints." *Materials & Design,* Vol. 128, (2017), 206-217, DOI:10.1016/j.matdes.2017.04.038.

22. Carloni, C., D'Antino, T., Sneed, L. H., Pellegrino, C. "Three-dimensional numerical modeling of single-lap direct shear tests of FRCM-concrete joints using a cohesive damaged contact approach." *Journal of Composites for Construction,* Vol. 22, No. 1, (2018), 04017048, DOI: 10.1061/(ASCE)CC.1943-5614.0000827.

23. D'Antino, T., Colombi, P., Carloni, C., Sneed, L. H. "Estimation of a matrix-fiber interface cohesive material law in FRCM-concrete jonts." *Composite Structures,* Vol. 193, (2018), 103-112, DOI:10.1016/j.compstruct.2018.03.005.

24. Zo, X., Sneed, L. H., D'Antino, T., Carloni, C. "Analytical Bond-SlipModel for Fiber-Reinforced Cementitious Matrix-Concrete Joints Based on Strain Measurements." *Journal of Materials in Civil Engineering,* Vol. 31, No. 11, (2019), 04019247, DOI: 10.1061/(ASCE)MT.1943-5533.0002855.

25. ACI (American Concrete Institute). Report on High-Strength Concrete. ACI 363 R. (2010). Farmington Hills, MI: ACI.

26. ABAQUS 6.14 [Computer software]. Dassault Systemes, Waltham, MA.

27. Genikomsou, Aikaterini S., and Maria Anna Polak. "Finite element analysis of punching shear of concrete slabs using damaged plasticity model in ABAQUS." *Engineering Structures,* Vol. 98, (2015), 38-48, DOI:10.1016/j.engstruct.2015.04.016.

28. Desayi, Prakash, and S. Krishnan. "Equation for the stress-strain curve of concrete." *Journal Proceedings*, Vol. 61. No. 3. 1964.

Persian Abstract

چکیده

سازه های بتونی مقاوم در برابر ماتریس سیمانی تقویت شده با الیاف (FRCM) به دلیل عملکرد مکانیکی و دوام بسیار گسترده شده اند. با این حال ، رفتار اعضای بتن آرمه تقویت شده با FRC تحت بارهای سرویس هنوز نگران کننده است و باید تلاش های بیشتری انجام شود. در این مطالعه ، یک مدل غیر خطی المان محدود سه بعدی (FE) برای مطالعه عملکرد تیرهای RC تقویت شده توسط FRCM ساخته شده است. مدل در برابر نتایج تجربی جمع آوری شده از شش پرتو آزمایش شده تحت خمش سه نقطه ای تأیید شد. در نتیجه ، پارامترهای اولیه عددی مورد مطالعه نسبت تقویت طولی فولاد و مقاومت فشاری بتن بودند. پارامترهای آسیب منسجم برای نشان دادن نتایج تجربی مورد بررسی قرار گرفت. همچنین ، ظرفیت خمشی نظری تیرهای تقویت شده بر اساس کد ACI-549.4R بر اساس نتایج روش عددی ارزیابی شد. به عنوان یک نتیجه گیری ، نتایج عددی در مورد بازده بار ، بار نهایی و حالت خرابی با نتایج تجربی مطابقت بسیار خوبی دارند. علاوه بر این ، مدلهای توسعه یافته از مطالعات پارامتریک تأثیر ناچیز مقاومت فشاری بتن بر افزایش ظرفیت نهایی تیر تقویت شده را نتیجه گرفتند. با این حال ، نسبت تقویت فولاد تأثیر عمده ای در افزایش ظرفیت نهایی تیرهای تقویت شده دارد.